Statistical Search for Migrations of Aftershock Sequences

AUTHOR(S):

IMOTO, Masajiro; KISHIMOTO, Yoshimichi

CITATION:

IMOTO, Masajiro ...[et al]. Statistical Search for Migrations of Aftershock Sequences. Bulletin of the Disaster Prevention Research Institute 1977, 27(3): 93-111

ISSUE DATE:

1977-09

URL:

http://hdl.handle.net/2433/124872

Bull. Disas. Prev. Res. Inst., Kyoto Univ., Vol. 27, Part 3, No. 249, September, 1977

Statistical Search for Migrations of Aftershock Sequences

By Masajiro IMOTO and Yoshimichi KISHIMOTO

(Manuscript received October 3, 1977)

Abstract

Aftershock sequences in Kuril of August 11, 1969 and June 17, 1973 are investigated by a statistical method. On the assumption of a unilateral propagation of aftershock activity, the direction of propagation is likely to be normal to the trench axis. On the basis of this result, time-space plots of other sequences in Kuril are examined. It is commonly observed that a quiescent area of aftershock activity originates at the epicenter of the main shock, and spreads seaward with time. The spreading velocity of a quiescent area is estimated at 8~16 km/day.

1. Introduction

For many years, many investigations have been done regarding aftershock phenomena, such as the frequency of aftershocks with time, Gutenberg-Richter's law (b values), seismicity maps, and so on. Recently, closer researches[1),2)] on seismicity maps have been made by more accurate data of hypocentral parameters. An aftershock area is considered to indicate the fracture zone of the main shock[3)]. On this assumption, maps of aftershocks play important roles for determining fault geometries and other source parameters. Also, the location of the main shock with respect to the aftershock area gives a hint on faulting characteriscics.

Kellher *et al.*[4)] examined aftershock areas of some large earthquakes at the trenches of the Pacific Ocean and the Caribbean Sea, and tried to forecast locations of large shallow earthquakes in near future. It was mentioned that epicenters of the main shocks tended to be located near the landward side of the aftershock area, and they inferred that during large thrust earthquakes ruptures initiate at some depth and propagate upward and seaward. We[5)] also examined relations between epicenters of the large thrust earthquakes and their aftershock areas using more recent and accurate data. Generally speaking, samely as one of their conclusions, epicenters of the main shocks are situated landward. But strictly, this tendency seems to be somewhat different for different regions, that is, this tendency is prominent in Kurll and not in New Britain and New Hebrides.

Mogi[6)] investigated development of aftershock areas of some great earthquakes which occurred in the Circum-Pacific Seismic Belt. Development of aftershock areas were seen during one year after main shocks. In the same paper, rapid propagations of aftershock activities were reported for the Alaskan Earthquake of March 28, 1964 and the Aleutian Earthquake of Marth 9, 1957. Ida[7)] proposed a model of slow-moving

disturbance of deformation to interpret the observed propagation of earthquake foci and nonseismic creep. His analysis was based on an assumption that thin fault gouge participates in viscous slip. The viscosity of the gouge was estimated from observed propagation speed. Investigations on the aftershock migration might give some rheological information in the source region.

In this paper, we investigate migration phenomena of aftershock sequences particularly in Kuril. Because, in this region, the seismic activity is high, many sequences with recent and accurate data of hypocenters are available, and aftershock activity is characterized by its large scale.[8] As mentioned in our paper cited above,[5] the relation between the epicenter of a main shock and its aftershock area, which is considered to be a distinctive feature of thrust faults, also holds good. These characters of the Kuril region are adequate to examine the aftershock activity systematically.

2. Data

We selected the sequences in which magnitude of main shocks are greater than 7, and each of which consisted of many shocks. These main shocks are listed in Table 1 and plotted in Fig. 1. The data of hypocentral coordinates, origin times, and magnitudes are after NOAA Earthquake Data File and Earthquake Data Report.

Magnitude-frequency relations were examined for two sequences of October 1963 and August 1969 so as to see detection capability for these sequences. All

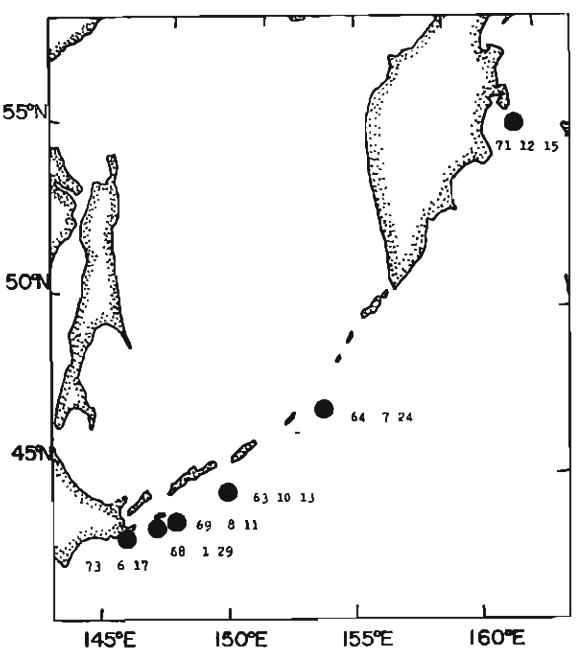

Fig. 1. Plots of the main shocks in Table 1.

Table 1. List of main shocks.

Date Y	M	D	Origin Time h	m	s	Epicenter Lat.°N	Lon.°E	Depth (km)	Mag.
63	10	13	5	17	57.1	44.8	149.5	60	8.1
64	7	24	8	12	40.0	47.2	153.8	33	7.0
68	1	29	10	19	5.6	43.6	146.7	40	7.0
69	8	11	21	27	39.4	43.5	147.4	28	7.8
71	12	15	8	29	55.3	56.0	163.3	33	7.8
73	6	17	3	55	2.9	43.2	145.8	48	7.7

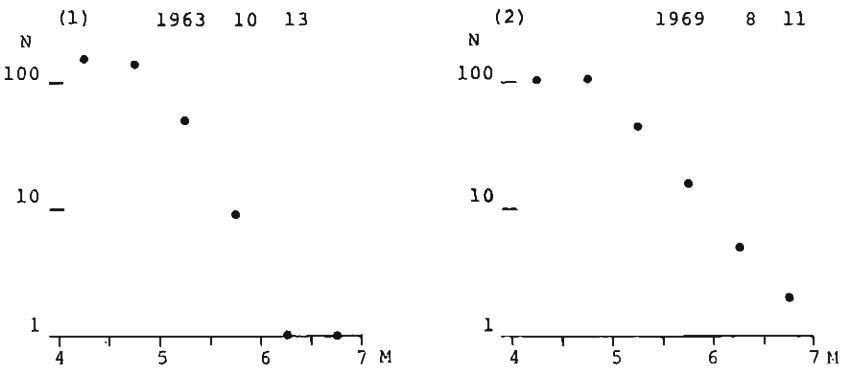

Fig. 2. Magnitude-frequency relations of October 1963 and August 1969 sequences.

aftershocks that occurred during 30 days after the main shock and within 200 km distance from it were adopted in both of Fig. 2 (1) and (2). Gutenberg-Richter's law seems to hold good in a range of magnitude greater than 4.5 for both sequences. We must take care to use data of smaller aftershocks. For the statistical analysis in later sections, we shall use the data of shocks with magnitudes greater than 4.5.

3. Time-space analyses of aftershock sequences

Time-space plots (figures with time and space axes) are often useful to see time variation of seismic active area. These plots sometimes give a good idea for investigations on seismic activity. However, space distribution of earthquakes in three dimensions is usually projected onto a line, and difference of direction of the line sometimes makes a quite different impression. What direction should be selected to obtain the best feature for representing physical meanings? We shall investigate the time variations of aftershock areas by the following statistical method and show how we can find the best direction of the projection line.

3.1 Method

Seismic activity is represented by the five parameters, origin time, hypocenter coordinates, and magnitude. Among these five parameters, time-space interaction is

important to see time variation of an aftershock area. If earthquakes in one sequence show propagative activity exactly in one direction, the apparent velocity between every two earthquakes

$$v_{ij}=\Delta x_{ij}/\Delta t_{ij}$$

where

Δx_{ij}: distance interval between **event** i and j

Δt_{ij}: time interval between **event** i and j,

will be equal to the speed of propagation. The $\Delta x_{ij}-\Delta t_{ij}$ relationship may give a hint for aftershock migrations.

Kagan and Knopoff[9] investigated a time-space-magnitude relationship among worldwide earthquakes of magnitudes greater than 7 by a statistical method. They assumed that earthquakes have a Poissonian distribution and compared the actual rate of occurrence of subsequent shocks in any time interval with the value calculated from the Poissonian. They examined the propability of occurrence of earthquakes actually obtained in each time-distance interval. According to them, some of these time-distance intervals in which earthquakes occurred much more frequently than expected by the Poissonian rate are explainable by the time-space relationship of a migration.

We do not assume any stochastic process such as Poisson process in their case to be compared with any actual process, but it is assumed that spatial distribution is independent of time. We examined how much inconsistency will occur on this assumption. The propability density of aftershock occurrence, $\rho(\boldsymbol{x}, t)$, is assumed to be the following,

$$\rho(\boldsymbol{x}, t)=\rho_1(\boldsymbol{x})\cdot\rho_2(t) \tag{1}$$

Integrating this function with respect to time in a certain period, a spacial distribution is obtained. In the same way, integrating with respect to space within a certain volume, a time-frequency relation is obtained. Distributions of pairs in relation to a certain time-distance interval, $\varphi(\Delta\boldsymbol{x}, \Delta t)$, are derived from $\rho(\boldsymbol{x}, t)$, as follows;

$$\varphi(\Delta\boldsymbol{x}, \Delta t)=\iint_{V\,T}\rho(\boldsymbol{s}, u)\cdot\rho(\boldsymbol{s}+\Delta\boldsymbol{x}, u+\Delta t)\,du\,d\boldsymbol{s}. \tag{2}$$

Substituting Eq. (1) into Eq. (2), we have

$$\begin{aligned}\varphi(\Delta\boldsymbol{x}, \Delta t)&=\iint_{V\,T}\rho_1(\boldsymbol{s})\cdot\rho_1(\boldsymbol{s}+\Delta\boldsymbol{x})\cdot\rho_2(u)\cdot\rho_2(u+\Delta t)\,du\,d\boldsymbol{s}\\&=\int_V\rho_1(\boldsymbol{s})\cdot\rho_1(\boldsymbol{s}+\Delta\boldsymbol{x})\,d\boldsymbol{s}\int_T\rho_2(u)\cdot\rho_2(u+\Delta t)\,du.\end{aligned} \tag{3}$$

Assuming that a domain V is so large that

$$\rho_1(\boldsymbol{s})=0$$

outside V,

$$\varphi(\Delta x,\ \Delta t) = \varphi(-\Delta x,\ \Delta t) \qquad (4)$$

is derived from Eq. (3). This equation means that a distribution of pairs in relation to Δx is expected to be symmetric with respect to the origin in any time interval Δt. In practice, integrals are replaced by summations. Aftershocks adopted in later analysis will be restricted to a certain domain V, so that the above assumption, $\rho_1(s) = 0$ outside V, shall be accepted.

Examples of symmetric and disturbed cases are seen in Fig. 3 (1) and (2).

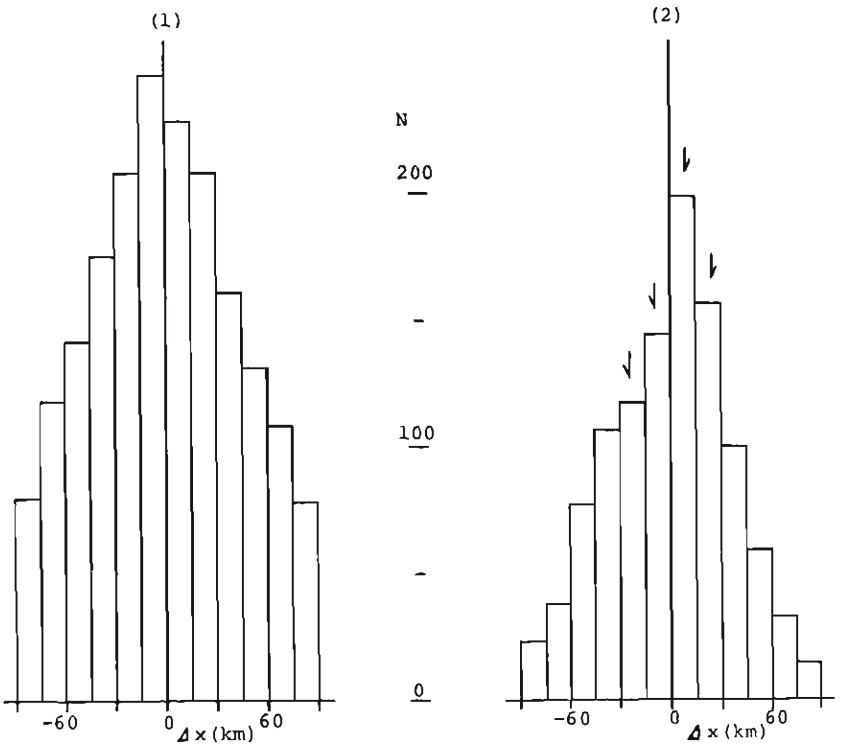

Fig. 3. Histograms of pairs in a certain time interval. (1) An example of symmetric case, (2) an example of disturbed case. Arrows indicate distance intervals of disturbance.

These are the histograms of pairs at every 15 km intervals and a certain range of time intervals ($\Delta t-\delta \sim \Delta t+\delta$). In Fig. 3 (2) (a disturbed case), symmetry is disturbed near $\Delta x = 15$ km or -15 km (indicated by arrows), that is, pairs in the distance intervals of $\Delta x = 0 \sim 15$ and $15 \sim 30$ km are more frequent than those in the corresponding intervals of $\Delta x = 0 \sim -15$ and $-15 \sim -30$ km. We may suspect that this excess of pairs in $\Delta x = 0 \sim 30$ km is caused by propagation of activity and that the velocity of propagation will be nearly equal to the apparent velocity, $\Delta x/\Delta t$.

3.2 Aftershock sequence of August 1969

The hypocentral parameters of the main shock are given in Table 1. Fault parameters were calculated by Abe.[10] The fault-plane solution is shown in Fig. 4. Abe concluded that the actual dislocation took place over a gently dipping

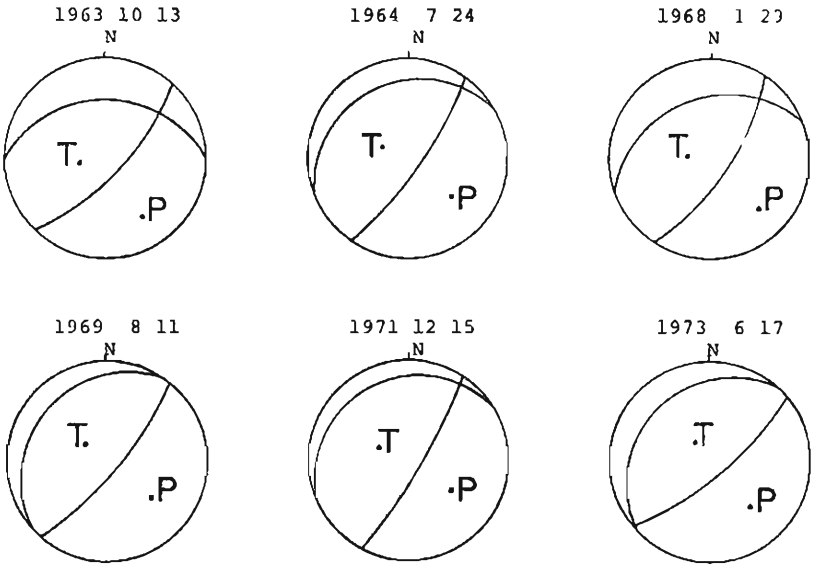

Fig. 4. Fault-plane solutions of the main shocks.[10),23)]

nodal plane, considering a large aftershock area and slip directions of neighboring earthquakes. Hatori[11] estimated source area of tsunami generated by this shock. This agreed with the aftershock area. One of the present authors[12] reported that just before the main shock, a few large foreshocks occurred and migrated to landward side of the aftershock area where the main shock took place. Motoya[13] investigated the aftershock activity with the data observed by sensitive seismographs at Urakawa and reported that the decay of frequency of aftershocks with time is well represented by an equation $n(t)=A\cdot(t+c)^{-p}$ ($p=1.0$, $c=0.02$ days). Santo[8] pointed out the migration of this sequence. We have investigated the aftershock activity of this sequence in more detail by the method mentioned above.

Fig. 5-(4) shows the epicenter distribution of the aftershocks during 20000 minutes (about 2 weeks) after the main shock. From these aftershocks, we selected about 120 shocks which occurred within 100 km distance from the main shock in both directions normal and parallel to the trench axis, and whose magnitudes are greater than 4.5. The range of magnitudes greater than 4.5 seems to be relatively narrow, so that it does not seem necessary to take magnitude as a parameter. The focal depth is generally less accurate than horizontal coordinates, and also the change of

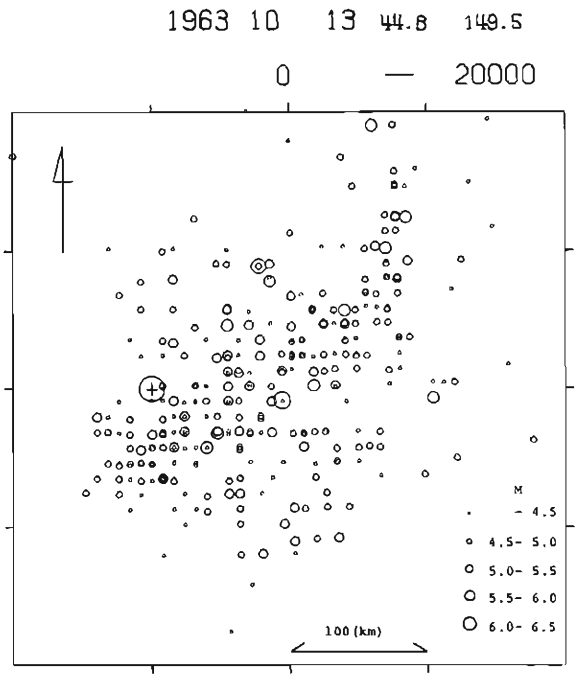
1963 10 13 44.8 149.5
0 — 20000
M
- 4.5
4.5- 5.0
5.0- 5.5
5.5- 6.0
6.0- 6.5
100 (km)

(1)

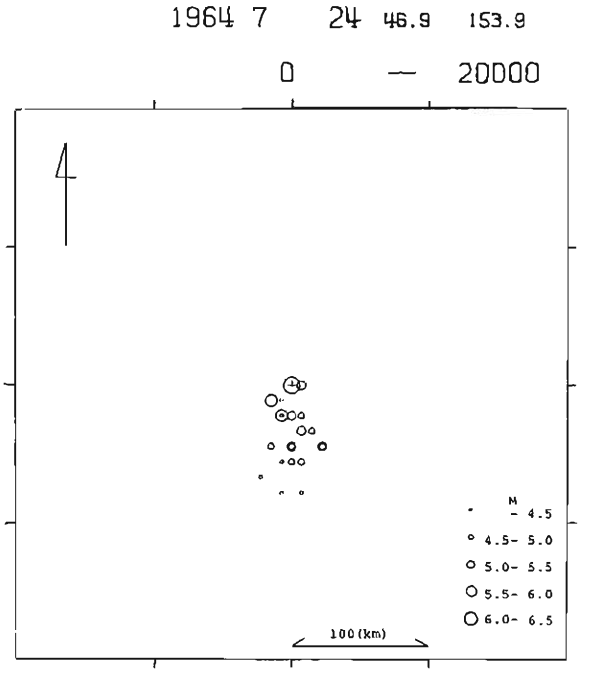
1964 7 24 46.9 153.9
0 — 20000
M
- 4.5
4.5- 5.0
5.0- 5.5
5.5- 6.0
6.0- 6.5
100 (km)

(2)

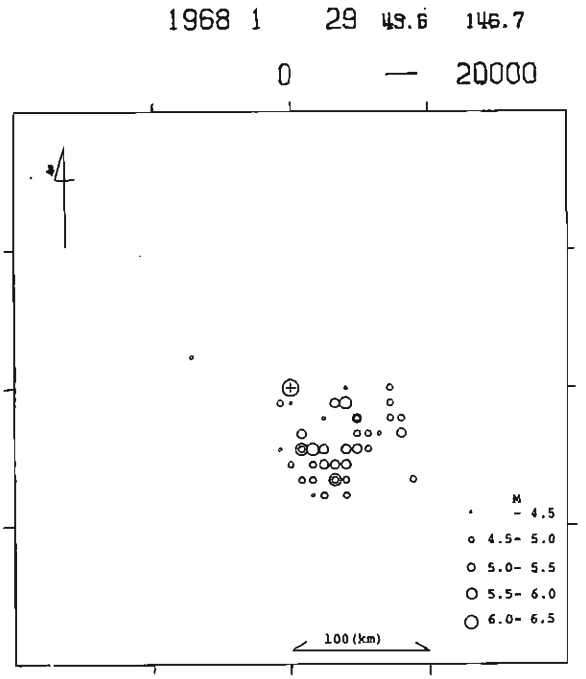
1968 1 29 43.6 146.7
0 — 20000
M
- 4.5
4.5- 5.0
5.0- 5.5
5.5- 6.0
6.0- 6.5
100 (km)

(3)

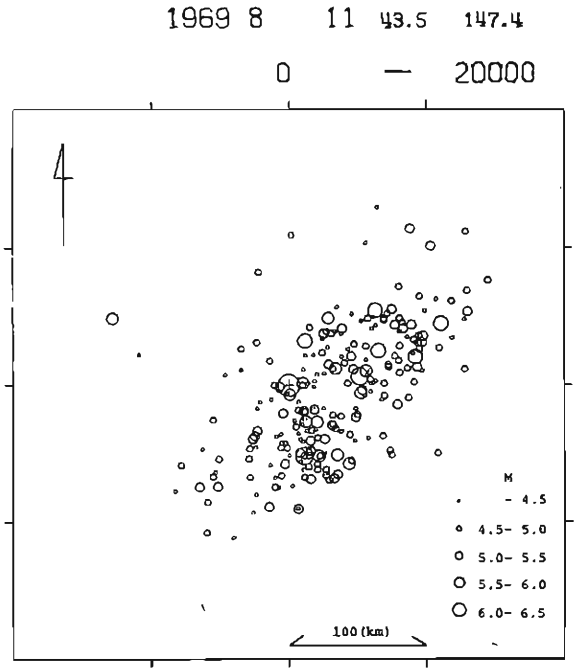
1969 8 11 43.5 147.4
0 — 20000
M
- 4.5
4.5- 5.0
5.0- 5.5
5.5- 6.0
6.0- 6.5
100 (km)

(4)

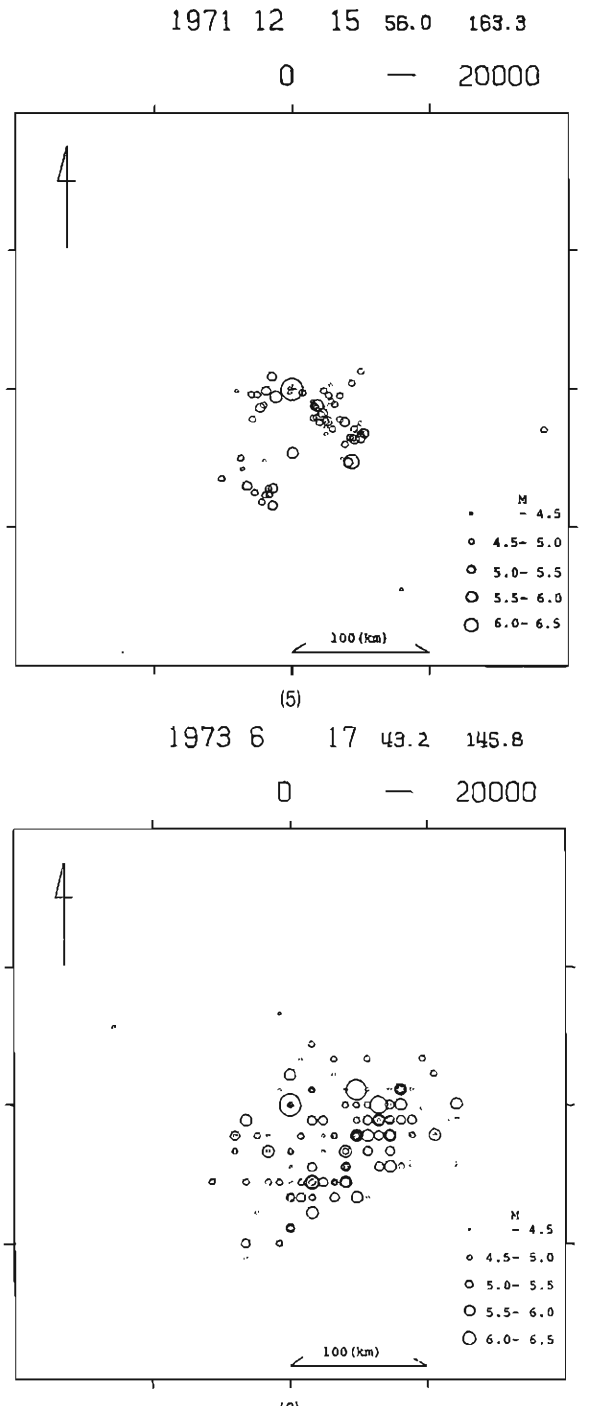

Fig. 5. Epicenters of aftershocks during 20000 minutes after the main shocks. The largest circle at a cross mark indicates the main shock.

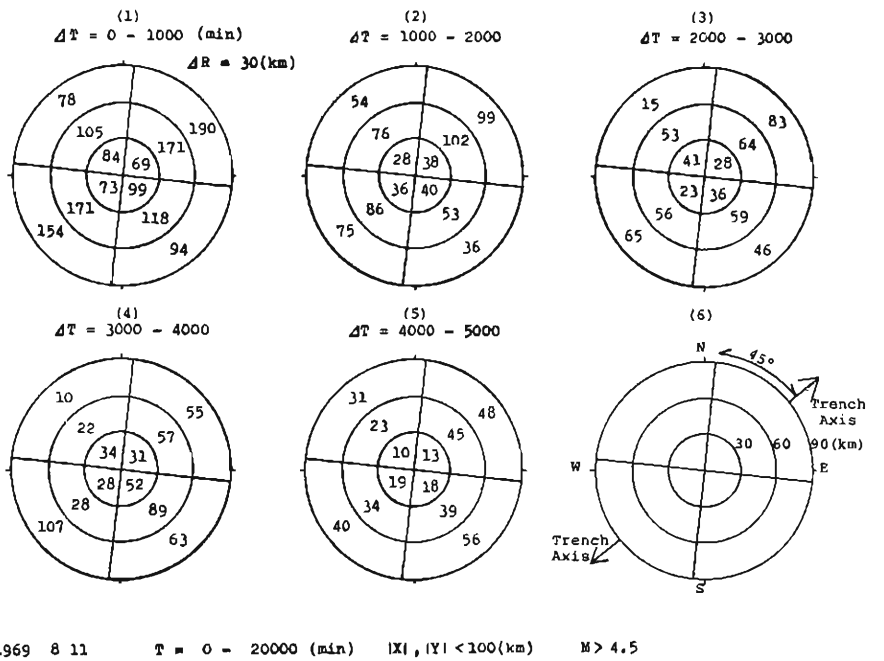

Fig. 6. Numbers of pairs in each time-space interval of August 1969 sequence. Coordinate system is referred to the trench axis as Fig. 6-(6).

focal depths seems to be rather small on the gently dipping fault plane. Therefore we use only three parameters of origin time and horizontal coordinates among the five parameters. The distributions of Δx are shown at successive 1000 minutes intervals in Fig. 6. As seen, Δx are represented by a polar coordinate system. The azimuth is classified into four quadrants, referring to the trench axis. Two rows of numerals from upper-right to lower-left and from upper-left to lower-right represent numbers of pairs parallel and normal to the trench axis, respectively. Fig. 6-(1) seems to show something symmetric with respect to the origin. On the other hand, in Fig. 6-(4), the distance intervals of 30~60 and 60~90 km have 22 and 10 pairs of NW direction and 89 and 63 pairs of SE direction, respectively. This figure does not show symmetry at all. This suggests that aftershock activity is apt to propagate in the SE direction (seaward). The ratio of NW−SE direction to total tends to increase with time, that is 41.1, 39.7, 44.0, 46.9, and 47.1(%). This means that shocks during short time intervals after any shock are apt to occur in NE−SW direction, and that with increase of time interval, activity of NW−SE direction, particularly SE direction becomes high.

Next, we estimate the speed and direction of migration. We used three parameters of (Δx, Δt) above. Hereafter we use only two parameters of (Δx, Δt) by projecting vector Δx on one line. An example is seen in Table 2. The line of projection is oriented in S40°E (positive) −N40°W (negative) direction. In every time-distance interval each entry is a ratio of the number of pairs in positive

Table 2. An example of time-space analysis of August 1969 sequence. Abscissa is time interval from one shock to another later shock, and ordinate is distance interval from the former of the pair to the later along S40°E (positive)-N40°W (negative) direction. Each entry indicates the ratio of number of pairs in positive direction to the total of both directions. Numbers with brackets are the total values. In the case that a hypothesis, a ratio is equal to 0.5, is rejected, the entry is underlined.

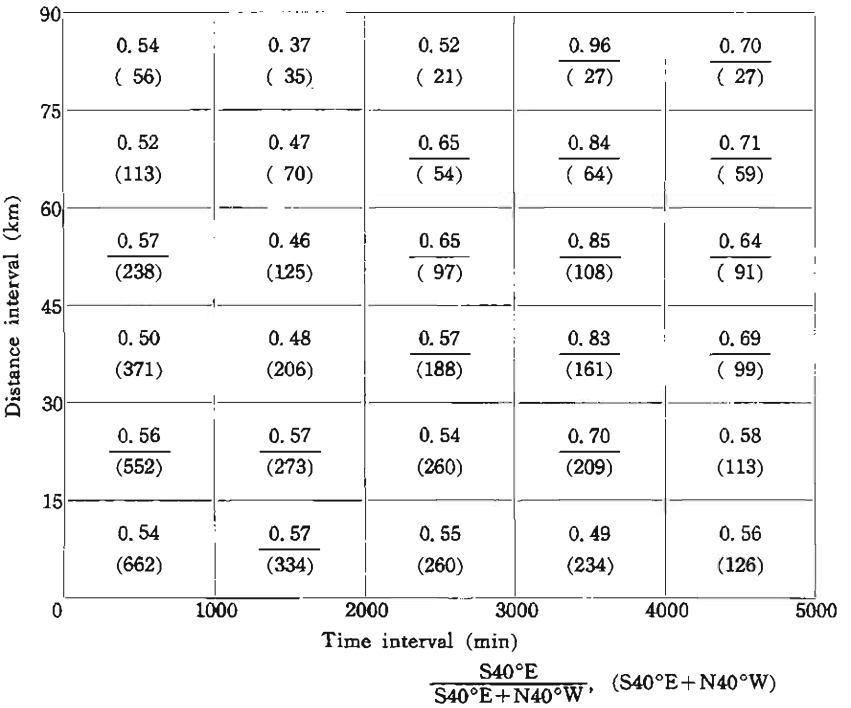

direction to total of both directions (the same distance interval but opposite direction). The total number is also shown with brackets in each interval. This ratio is an indicator of the symmetry, and is expected to be 0.5 in a symmetric case. With some exceptions, the ratio is larger than 0.5 in Table 2. Under a null hypothesis that both directions have the same propability (0.5), the binominal test is used at the level of significance of 5%. The entry is underlined in the case that this hypothesis is rejected. As we examine these underlined entries, it seems that the asymmetric case takes place in farther distance interval with increase of time interval. This might show the seaward propagation of aftershock activity. We estimate the speed at 10~35 km/day.

Fig. 7 shows the results concerned with other directions of projection lines. The direction of the line is set for every 30 degrees from parallel to the trench axis. The six lines in the figure show these directions. They intersect at the epicenter of the main shock. The longer part of each line shows the positive direction in projection. Six inserted figures are obtained in the same way as Table 2, ordinate

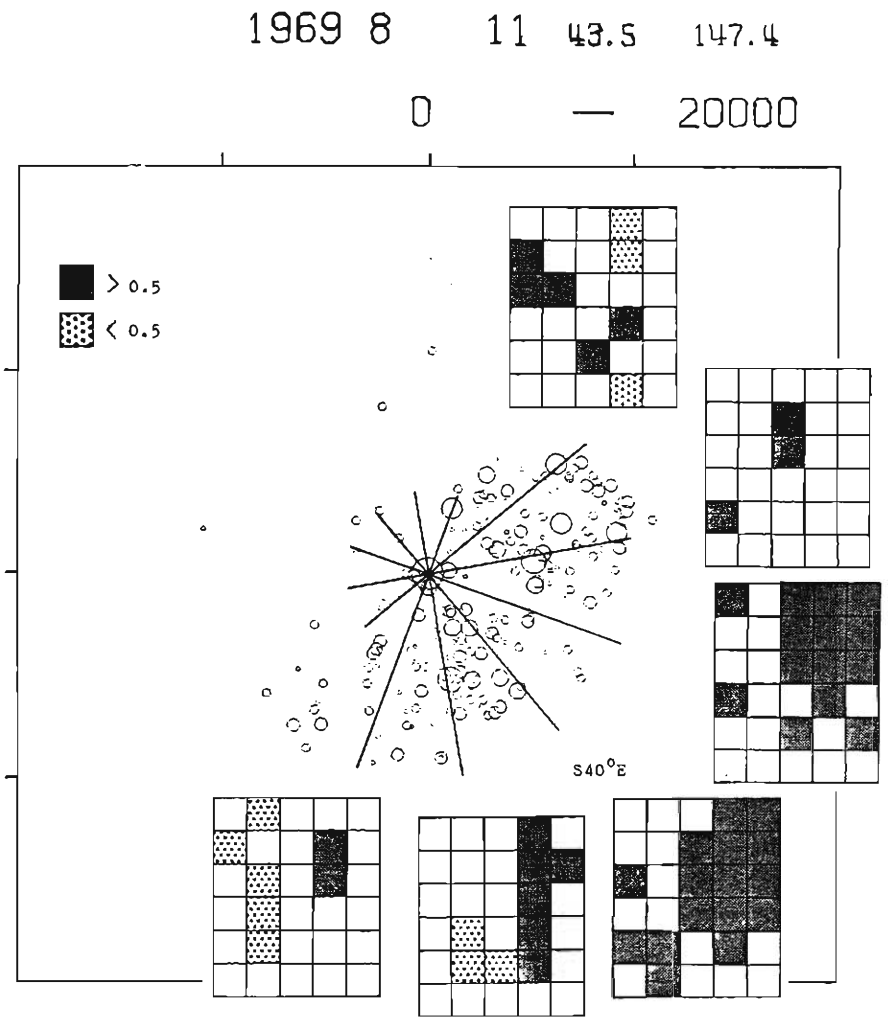

Fig. 7. Results of time-space analysis of August 1969. Six lines indicate directions of projection. Inserted figures are results of analysis in respective directions of projection. Ordinate and abscissa are graduated in every 15 km of distance interval and 1000 minutes of time interval, respectively. A black block shows that a ratio of the number of pairs in positive direction to the total of both directions is expected to be greater than 0.5 by a binominal test. A dotted block shows that a ratio is to be smaller than 0.5. A blank block shows the other case. Epicenters of aftershocks are also shown (see Fig. 5-(4)).

and abscissa are graduated in every 15 km of distance interval and 1000 minute of time interval, respectively. The binominal test was used in each time-distance interval, and the result is represented in three ways as follows: A blank means that null hypothesis is not rejected. The black means that the hypothesis is rejected and that

the propability of positive direction is expected to be larger than 0.5. The dotted means that the hypothesis is also rejected and that the propability is to be smaller than 0.5. As seen in Fig. 7, the symmetry is largely disturbed in the cases of S70°E and S40°E directions. If we assume that the migration is one directional, or unilateral, the direction is most likely to be normal to the trench axis or somewhat counterclockwise. The speed is estimated at 10-35 km/day as before.

3.3 Aftershock sequence of June 1973

This earthquake occurred on June 17, 1973 in eastern Hokkaido. It had been predicted on the basis of a seismicity gap.[14] The faulting nature of this earthquake is considered to be similar to those of neighboring great earthquakes (see Fig. 4),

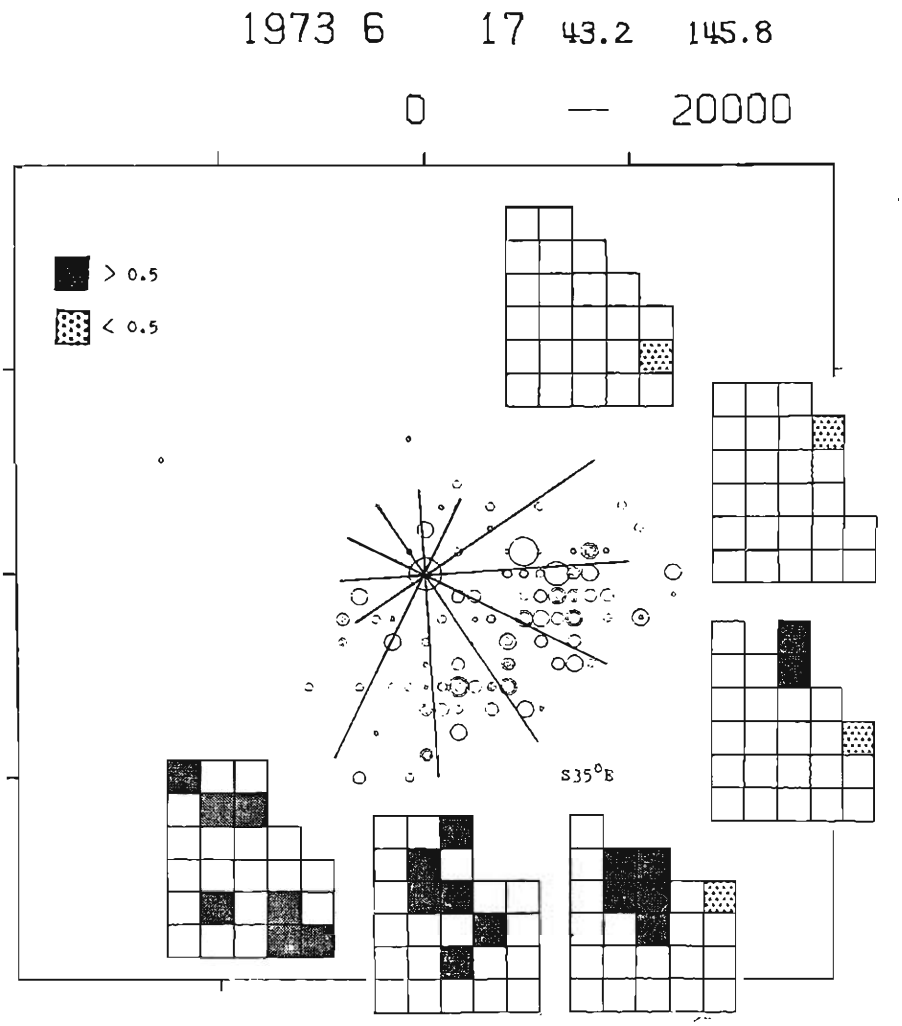

Fig. 8. Results of time-space analysis of June 1973. Notations are the same as those of Fig. 7.

but in quantity this shock was smaller by a factor of 3～5[15),18)] than the earthquake in the previous section. The epicenters of aftershocks are plotted in Fig. 5-(6). Number of aftershocks is smaller than that of the previous case. In the same way as the previous, we investigate migration of this sequence. The results are shown in Fig. 8 with the same notations as those in Fig. 7. The upper-right parts of inserted figures are cut off because of scanty data. It seems that the symmetry is most largely disturbed in the direction normal to the trench axis. It might be concluded that the direction of propagation, on the assumption of unilateral propagation, is seaward. The speed of the propagation is estimated at 20－50 km/day.

3.4 Time-space plots of sequences

In Kuril, many large earthquakes occurred recently. Among them, the shocks followed by many aftershocks are listed in Table 1. These have been already investigated by many authors.[17)-23)] These main shocks are situated on landward side of their aftershock areas (see Fig. 5). The fault-plane solutions are given in Fig. 4. These shocks seem to be of the similar faulting nature, for example, a low angle thrust fault.

Fig. 9 shows time-space plots of those sequences, where epicenters of shocks are projected on a line normal to the trench axis. Ordinate and abscissa indicate the distance from, and the time lapse after the main shock, respectively. Each of Fig. 9 (1)-(6) shows a migration feature well. Particularly in Fig. 9 (2), (3) and (5), a quiescent area of activity originates at the epicenter of the main shock, and spreads seaward with time. Such a feature appears in the other cases, although it is not so clear. Spreading speeds are 8－16 km/day.

4. Discussion and conclusion

One of the present authors[24)] has already reported such a migration feature of aftershock activities in other regions as those mentioned in the previous sections. A spreading speed of quiescent area is summarized in Table 3. These values were estimated visually from time-space plots such as Fig. 9. In each case of August 1969 and June 1973, the speed in Table 3 is lower than that estimated previously by the statistical method. Because the former represented a propagation velocity of relatively high seismicity, and the latter represented the velocity of lower limit. The difference between two values estimated by different methods is at most a fatcor 2～4. It may be concluded that the propagation speed of aftershock sequences in Kuril is the same order as that of San Fernand earthquake,[1)] and on the other hand much lower than those of Alaska and Aleutian sequences.[6)] In Kuril, the fault width of a large thrust earthquake is about 100 km, and propagation speed is about 10 km/day. Then, the migration should be observed during only about 10 days just after a main shock. Even if migrations are concerned in a crustal movement, it is difficult to detect this short time deformation by leveling. Tada[22)] reported crustal movement during a short period after the 1973 Nemuro-Oki Earthquake on the basis of tide

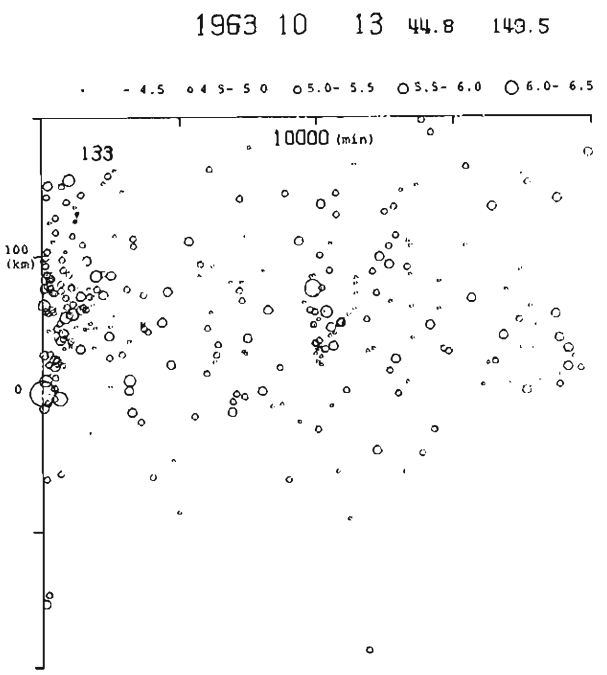
1963 10 13 44.8 143.5
- 4.5 4.5- 5.0 5.0- 5.5 5.5- 6.0 6.0- 6.5
10000 (min)
133
100 (km)
0

(1)

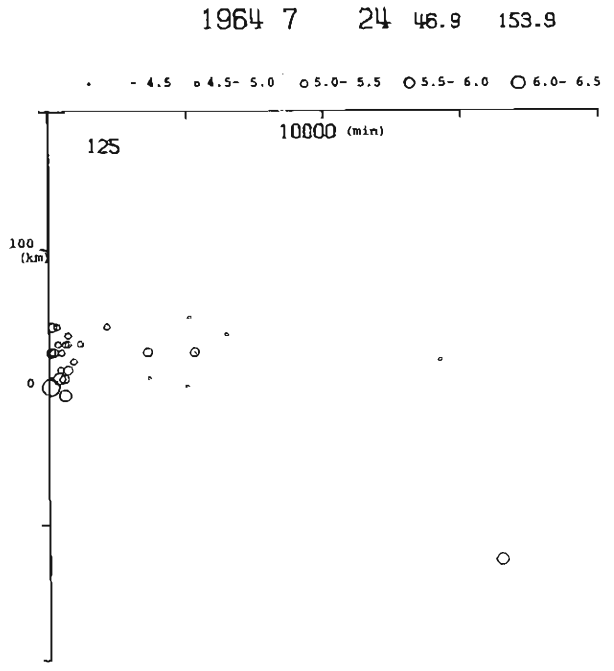
1964 7 24 46.9 153.9
- 4.5 4.5- 5.0 5.0- 5.5 5.5- 6.0 6.0- 6.5
10000 (min)
125
100 (km)
0

(2)

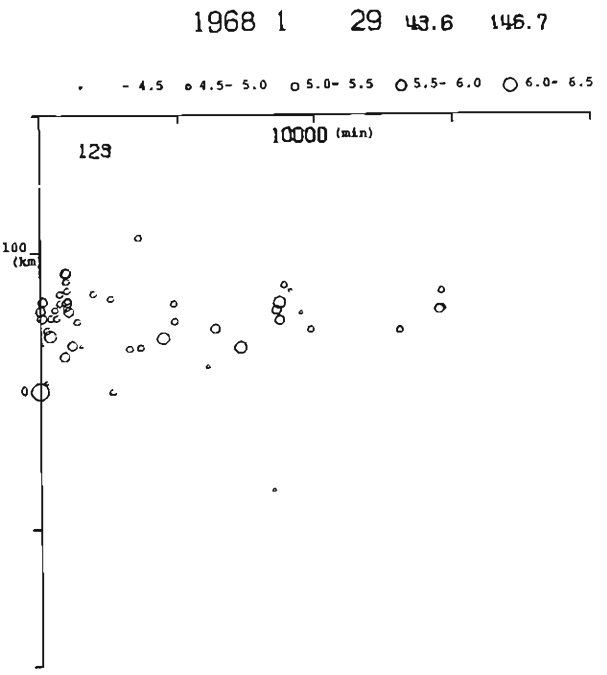
1968 1 29 43.6 146.7
- 4.5 4.5- 5.0 5.0- 5.5 5.5- 6.0 6.0- 6.5
10000 (min)
129
100 (km)
0

(3)

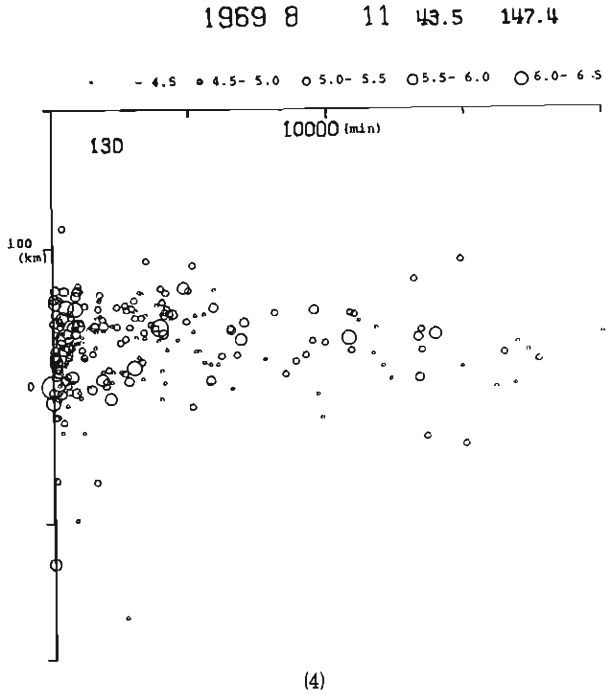
1969 8 11 43.5 147.4
- 4.5 4.5- 5.0 5.0- 5.5 5.5- 6.0 6.0- 6.5
10000 (min)
130
100 (km)
0

(4)

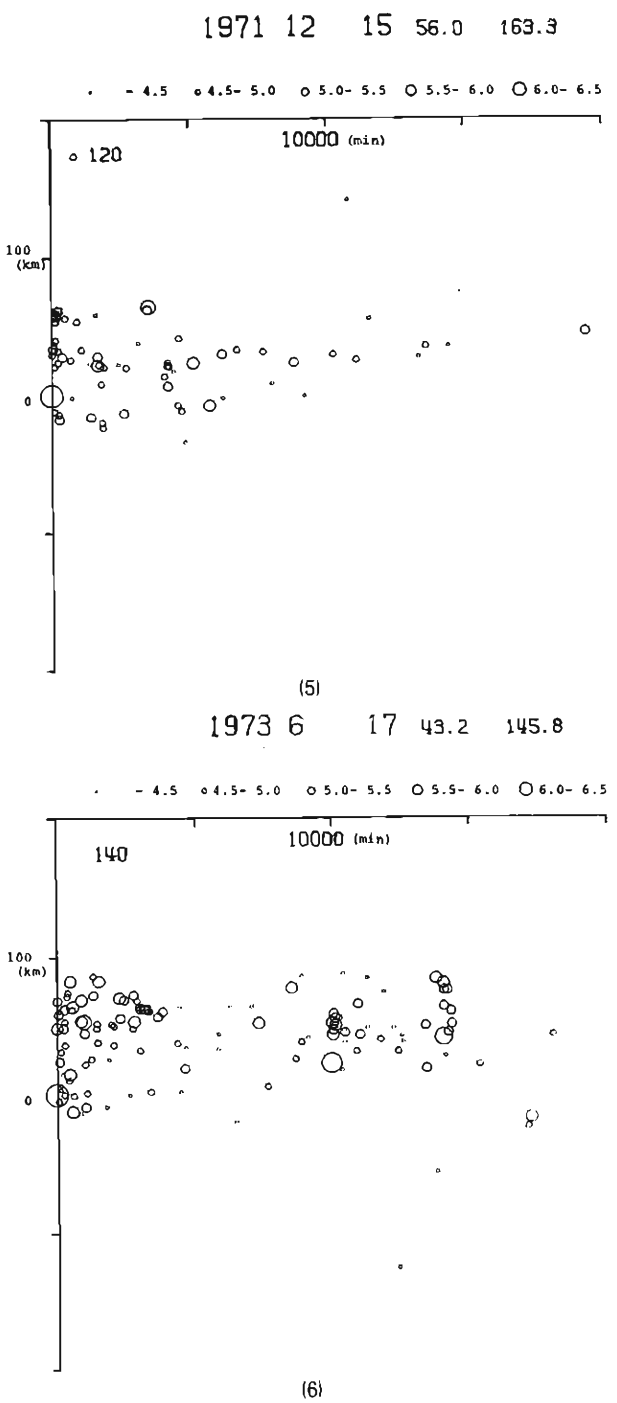

Fig. 9. Time-space plots of sequences. Ordinate and abscissa indicate the distance from and the time lapse after the main shock, respectively. The number at a upper-left corner is the azimuth of a projection line counted clockwise from the north.

Table 3. Spreading velocities of quiescent areas.

Date Y	M	D	Epicenter Lat.	Lon.	Velocity (km/day)
1970	4	29	14.5°N	92.6°W	11
1971	7	9	32.5°S	71.2°W	15
1972	12	2	6.5°N	126.6°E	7
1964	7	24	47.3°N	153.8°E	8
1968	1	29	43.6°N	146.7°E	8
1969	8	11	43.5°N	147.4°E	9
1971	12	15	56.0°N	163.3°E	9
1973	6	17	43.2°N	145.8°E	13

gauge records.

In any case, detailed researches for mechanisms of migrations are left for future study. Our conclusions summarized as follows:

1) On the assumption of unilateral propagation, the direction of propagation is likely to be normal to the trench axis.

2) Time-space plots, where epicenters of aftershocks are projected onto the line normal to the trench axis, show that the quiescent area starts at the epicenter of the main shock and spreads seaward.

3) Propagation speeds of aftershock sequences are estimated at 8~50 km/day.

Acknowledgement

We have been helped and advised by Mr. K. Matsumura and Mr. H. Noda in processing of the NOAA Earthquake Data File. We would like to thank the members of Microearthquake and Earthquake Prediction Sections of Disaster Prevention Research Institute, Kyoto University for their discussion and encouragement. The computations are processed by the use of the computer in Information Processing Center of Disater Prevention Research Institute.

References

1) Whitcomb, J. H., C. R. Allen, J. D. Garmany and J. A. Hileman: San Fernando Earthquake Series, 1971: Focal Mechanisms and Tectonics, Rev. Geophys. Space Phys., Vol. 11, 1973, pp. 693-730.

2) Yamakawa, N.: Aftershocks and Focal Mechanisms of Main shocks, Geophys. Mag., Vol. 36, 1972, pp. 15-30.

3) Kanamori, H.: Synthesis of Long-Period Surface Waves and Its Application to Earthquake Source Studies-Kurile Islands Earthquake of October 13, 1963-, J. Geophys. Res., Vol. 75 No. 26, 1970, pp. 5011-5027.

4) Kelleher, J., L. Sykes and J. Oliver: Possible Criteria for Predicting Earthquake Locations and Their Application to Major Plate Boundaries of the Pacific and the Caribbean, J. Geophys. Res., Vol. 78 No. 14, 1973, pp. 2547-2585.

5) Imoto, M. and Y. Kishimoto: On a Bias of Aftershock Epicenters at Trenches of the

Pacific Ocean, Disas. Prev. Res. Inst. Kyoto Univ. Annuals, No. 20, 1977, (in Japanese, in preparation).

6) Mogi, K.: Development of Aftershock Areas of Great Earthquakes, Bull. Earthquake Res. Inst. Tokyo Univ., Vol. 46, 1968, pp. 175-203.
7) Ida, Y.: Slow-Moving Deformation Pulses along Tectonic Faults, Phys. Earth Panet. Inter., Vol. 9, 1974, pp. 328-337.
8) Santo, T.: Regional Study on the Characteristic Seismicity of the World. Part VII. -Activity of Aftershocks in Kuril Islands Region-, Bull. Intern. Inst. Earthq. Engin., Vol. 7, 1970, pp. 119-131.
9) Kagan, Y. and L. Knopoff: Statistical Search for Non-Random Features of the Seismicity of Strong Earthquake, Phys. Earth Planet. Inter., Vol. 12, 1976, pp. 291-318.
10) Abe, K.: Tsunami and Mechanism of Great Earthquake, Phys. Earth Planet. Inter., Vol. 7, 1973, pp. 143-153.
11) Hatori, T.: An Investigation of the Tsunami generated by the East Hokkaido Earthquake of August, 1969., Bull. Earthquake Res. Inst. Tokyo Univ., Vol. 48, 1970, pp. 399-412.
12) Imoto, M.: On a Starting Point of the Large Fracture of August 11, 1969 Hokkaido Toho-oki Earthquake, Zisin, Ser. II Vol. 29 No. 1, 1976, pp. 1-13 (in Japanese).
13) Motoya, Y.: Aftershock Sequence of the Earthquake East off Hokkaido on August 12, 1969, Geophys. Bull. Hokkaido Univ., Vol. 24, 1970, pp. 93-106 (in Japanese).
14) Utsu, T.: Large Earthquake near Hokkaido and the Expectancy of the Occurrence of a Large Earthquake off Nemuro, Rep. Coord. Comm. Earthquake Pre. Geogr. Surv. Inst., Vol. 7, 1972, pp. 7-13 (in Japanese).
15) Shimazaki, K.: Nemuro-Oki Earthquake of June 17, 1973: A Lithosheric Rebound at the Upper Half of the Inteface, Phys. Earth Planet. Inter., Vol. 9, 1974, pp. 314-327.
16) Hatori, T.: Tsunami Activity in Eastern Hokkaido after the Nemuro Peninsula Earthquake in 1973, Zisin, Ser. II Vol. 28 No. 4, 1975, pp. 461-471.
17) Santo, T.: Shock Sequence of the Southern Kurile Islands from October 09 to December 31, 1963, Bull. Intern. Inst. Seism. Earthq. Engin., Vol. 1, 1964, pp. 33-54.
18) Yamakawa, N., M. Kishio and K. Abe: Spacial and Time Distributions of Foreshocks and Aftershocks of the Earthquke near the Southern Kuril Islands on 13 October 1963, Geophy. Mag., Vol. 34 No. 3, 1969, pp. 277-306.
19) Maki, T.: Focal Mechanisms of the 1963 Itrup Earthquake Sequence, Geophys. Bull. Hokkaido Univ., Vol. 19, 1968, pp. 21-55 (in Japanese).
20) Hirota, T.: Aftershock Sequence of the Earthquake off Shikotan Island on January 29, 1968, Geophys. Bull. Hokkaido Univ., Vol. 21, 1968, pp. 93-106 (in Japanese).
21) Tada, T.: Fault Model and Crustal Movement of the 1973 Nemuro-Oki Earthquake, Zisin, Ser. II Vol. 27 No. 2, 1974, pp. 120-128 (in Japanese).
22) Tada, T.: Anelastic Recovering Fault Motion of Continental Plate Immediately after the 1973 Nemuro-Oki Earthquake, Zisin, Ser. 2 Vol. 27 No. 2, 1974, pp. 167-169 (in Japanese).
23) Stauder, W. and L. Mualchin: Fault Motion in the Large Earthquakes of the Kuril-Kamchatka Arc and of the Kuril-Hokkaido Corner, J. Geophys. Res., Vol. 81 No. 2, 1976, pp. 297-308.
24) Imoto, M.: Presented at the Spring Meeting Seism. Soc. Japan (14 May 1977).